A COMPARISON OF ACCURACIES OF THE RPC MODELS : HOMO- AND HETERO-TYPE STEREO PAIRS OF GEOEYE AND WORLDVIEW IMAGES

S. Y. Choi [a,*], J. M. Kang [b], D. S. Shin [a]

[a] 3ATRC-1, ADD, 111, Sunam-dong, Yuseong-gu, Daejeon, 305-152, Korea - (sychoi, dsshin)@add.re.kr
[b] Dept. of Civil Engineering, Chung-Nam National Uni., Yuseong-gu, Daejeon, 305-763, Korea - jmkang@cnu.ac.kr

Commission IV, WG IV/3

KEY WORDS: Accuracy, RPC Model, Homo-type stereo, Hetero-type stereo, GeoEye-1 images, WorldView-2 images

ABSTRACT:

We investigated the accuracy in three dimensional geo-positioning derived by two homo-type stereo pairs and four hetero-type stereo pairs of high resolution satellite images using the vendor-provided rational polynomial coefficients (RPC) in this research. The results of 3D geo-positioning from six different stereo combinations were assessed with seventeen GPS points which were commonly well distributed in the scenes. Recently, satellite image vendors provide homo-type stereo pair images taken by the same sensor during a short time period. Stereo pair images have good geometry for achieving accurate ground coordinates. However it is difficult to acquire them at the request time because of the revisit time of the satellite and current weather conditions. Due to these reasons, a new methodology using hetero-type stereo pairs has been suggested to derive ground coordinates. High resolution satellite images include the rational function model in the form of RPC which represents the relationship between the image coordinates and object coordinates with rational polynomials. RPC makes it fast, accurate, and simple to calculate ground coordinates without any exterior orientation parameters of satellites. We constituted six different stereo pairs from four images of GeoEye-1 in-track stereo pair images and WorldView-2 in-track stereo pair images which were collected for the same region (17.5km x 10.0km) of the west coast in Korea. We collected GCPs by differential GPS surveying. The ground coordinates derived from six different pairs without and with some GCPs were compared to all GPS points respectively. The accuracy of ground coordinates from hetero-type stereo pairs is equivalent to the accuracy from homo-type stereo pairs. This research demonstrates that we can achieve comparatively accurate ground coordinates without GCPs using any stereo combinations of images containing proper RPCs, although we don't have in-track stereo pair images. Furthermore, some proper combinations of images with GCPs can improve the positioning accuracy.

1. INTRODUCTION

Since IKONOS was launched in 1999 and provided publicly available high-resolution imagery at 1- and 4-meter resolution, high resolution satellite imagery has become indispensible for aspects of various areas such as urban management, large scale map development, etc.

Recently GeoEye-1 and WorldView-2 satellites have provided high resolution (0.5m) in-track stereo-pair images. As in-track stereo pair is taken from two different perspectives during one orbital pass, in-track stereo data acquisition has a strong advantage over multi-date cross-track stereo data acquisition. It reduces radiometric image variations (temporal changes, sun illumination, etc.), and thus increases the correlation success rate in any image matching process (Toutin, 2004).

In addition, when using high resolution satellite imagery for topographic mapping, in-track stereo pair images can ensure the geometric accuracy of generated DSM. However with respect to spatial information collection, the limitation such as expensive data acquisition fee, insufficiency of imaging regions and archived data is apparent (Zhu, 2008). Provided the images acquired from various satellite sensors are available, the full exploitation of these images will extend the possibility of spatial information collection, cut down expenses, and save time to prepare taking photographs.

Most of recent satellite images such as GeoEye-1 and WorldView-2 images provide a rational polynomial coefficient (RPC) model which is a kind of generic sensor model that is widely used in the processing of high-resolution satellite images. Unlike traditional physical camera models, an RPC model has 80 coefficients and simulates the sensor's position, attitude, and interior orientation, so the RPC model has no physical interpretation and is applicable to any images regardless of an acquisition sensor. This means hetero-type stereo pairs can be used for determining the precise position. In this paper, there are two kinds of stereo pairs. One is homo-type stereo pairs that is a stereo model using stereo pairs acquired from the same sensor, and the other is hetero-type stereo pairs that is a stereo model using stereo pairs acquired from different sensors.

There have been not many studies for regarding the application of high resolution satellite hetero-type stereo pairs. Zhu investigated the geometric accuracy of DSMs and orthoimages, which were obtained from homo-type and hetero-type stereo pairs of four IKONOS and two QuickBird panchromatic images, in 2008.

In this study, two kinds of homo-type stereo pairs and 4 kinds of hetero-type stereo pairs were used to make RPC stereo models using in-track stereo pairs of GeoEye-1 images and in-track stereo pairs of WorldView-2 images. We investigated the accuracy in three dimensional geo-positioning without and with GCPs for each 6 stereo pairs. The stereo acquisition geometry of the stereo pairs is used to analyze the relationship between the geometric accuracy of the RPC model and the geometric parameter such as B/H (Base to Height) ratio, BIE (Bisector Elevation Angle), and CA (Convergence Angle) (Zhu, 2008, Tong, 2008). The results show that RPC models of any stereo pairs of high resolution satellite stereo images have the potential to be used for three dimensional geo-positioning.

2. DATASETS AND RPC MODELS

For this study, GeoEye-1 and WorldView-2 in-track stereo pairs covering the same area of the west coast of Korea were used. The test area covers both high and low altitudes. Table 1 shows the properties of the used satellite images.

Sensor	GeoEye-1		WorldView-2	
Image ID	GE_01	GE_02	WV_01	WV_02P
Product	Geo Stereo		Stereo 1B	
Scan direction	Reverse	Reverse	Reverse	Forward
Resolution	0.5m	0.5m	0.65m	0.51m
Azimuth	345.3°	219.2°	169.3°	104.8°
Elevation	68.7°	66.3°	51.6°	73.0°
Date(GMT)	2010.4.25 02:30	2010.4.25 02:31	2010.4.23 02:28	2010.4.23 02:27

Table 1. Properties of the used satellite images

Seventeen Ground Control Points (GCPs) were collected in the test area with 3cm in horizontal and 5cm in vertical accuracies. The GCPs were used as control points for RPC modeling and as check points for evaluating the geometric accuracy of RPC modeling. Figure 1 shows the configuration of the GCPs. The center point (#37) and the points (#9, #11, #61, #100) distributed in the boundary regions were used for control points respectively. All of the seventeen GCPs were acquired through Differential Global Positioning System (DGPS) processing. We painted white triangle-shaped marks on the black paved road, and collected GPS signals on the center of the mark.

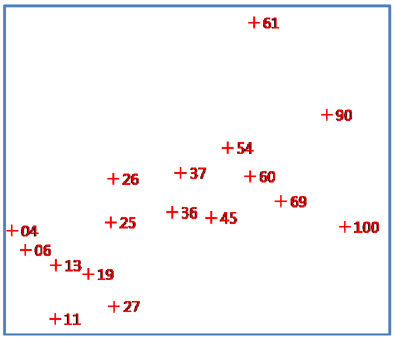

Figure 1. Configuration of GCPs

The RPC model used in this study proposed in Grodecki and Dial (2003) is briefly summarized here. The RPC model relates the object-space (φ,λ,h) coordinates to image-space (Line, Sample) coordinates. The RPC functional model is in the form of a ratio of two cubic polynomials of object-space coordinates. Separate rational functions are used to express the object-space to line and the object-space to sample coordinates relationship. To improve numerical precision, image- and object-space coordinates are normalized to (-1, 1) range using scales and offsets as shown below.

$$P = \frac{\varphi - \varphi_o}{\varphi_s} \quad (1)$$

$$L = \frac{\lambda - \lambda_o}{\lambda_s} \quad (2)$$

$$h = \frac{h - h_o}{h_s} \quad (3)$$

where φ_o: latitude offset, φ_s : latitude scale
λ_o: longitude offset, λ_s : longitude scale
h_o: height offset, h_s : height scale

The normalized line and sample image-space coordinates (Y and X, respectively) are then calculated from their respective rational polynomial functions g(.) and h(.): i.e.,

$$Y = g(\varphi,\lambda,h) = \frac{Num_L(P,L,H)}{Den_L(P,L,H)} = \frac{\mathbf{c'u}}{\mathbf{d'u}} \quad (4)$$

where

$\mathbf{u} = (1\ L\ P\ H\ LP\ LH\ PH\ L^2\ P^2\ H^2\ PLH\ L^3\ LP^2\ LH^2\ L^2P\ P^3\ PH^2\ L^2H\ P^2H\ H^3)'$

$\mathbf{c} = (c_1\ c_2 \cdots c_{20})'$

$\mathbf{d} = (1\ d_2 \cdots d_{20})'$

And similarly

$$X = h(\varphi,\lambda,h) = \frac{Num_S(P,L,H)}{Den_s(P,L,H)} = \frac{\mathbf{e'u}}{\mathbf{f'u}} \quad (5)$$

$\mathbf{u} = (1\ L\ P\ H\ LP\ LH\ PH\ L^2\ P^2\ H^2\ PLH\ L^3\ LP^2\ LH^2\ L^2P\ P^3\ PH^2\ L^2H\ P^2H\ H^3)'$

$\mathbf{e} = (e_1\ e_2 \cdots e_{20})'$

$\mathbf{f} = (1\ f_2 \cdots f_{20})'$

Using line and sample offsets and scale factors, the de-normalized image-space coordinates (Line, Sample), where Line is the image line number expressed in pixels with pixel zero as the center of the first line, and Sample is the sample number expressed in pixels with pixel zero as the center of the left-most sample, are finally computed as

$$Line = Y \cdot Line_s + Line_o \quad (6)$$

$$Sample = X \cdot Sample_s + Sample_o \quad (7)$$

where

$Line_o$: line offset, $Line_s$: line scale

$Sample_o$: sample offset, $Sample_s$: sample scale

Observation equation used is as below based image i and image point j.

$$F^i_{Lj} = -Line^i_j + a^i_0 + a^i_1 S_j + a^i_2 L_j + \frac{Num^i_{Lj}(P,L,H)}{Den^i_{Lj}(P,L,H)} \cdot L^i_s + L^i_o + \varepsilon^i_{Lj} = 0 \quad (8)$$

$$F^i_{Sj} = -Sample^i_j + b^i_0 + b^i_1 S_j + b^i_2 L_j + \frac{Num^i_{Sj}(P,L,H)}{Den^i_{Sj}(P,L,H)} \cdot S^i_s + S^i_o + \varepsilon^i_{Sj} = 0 \quad (9)$$

To validate modeling accuracy, the ground coordinates of the check points are initialized with the object space coordinates offset (φ_o,λ_o,h_o). We used horizontal object coordinates for uncertainty at 1.0e+5 for the check points and 1.0e-5 for the control points.
In the RPC block modeling, firstly we considered affine transformation for bias compensation as above equations (8) and (9), but we used shift transformation(a_1=a_2=b_1=b_2=0), because it is simple and there are no significant differences between the results of shift transformation and affine transformation through several experiments.

3. ACCURACY ANALYSIS OF STEREO MODELS

The geometries of GeoEye-1 images and WorldView-2 images are shown in Figure 2. The geometry of stereo images collected in in-track orbit is usually good for 3D geo-positioning. In Figure 2, the azimuths of GE_01 and GE_02 images and WV_01 and WV_02 images are 345.3°, 219.2°, 169.3°, and 104.8°, and the elevation angles of those images are 66.3°, 68.7°, 51.6°, and 73.0° respectively. Any combination of stereo image pairs has good geometry to perform geolocation via spatial intersection.

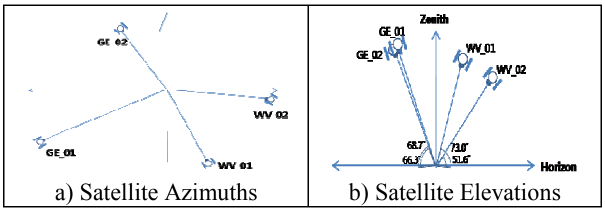

Figure 2. Image Geometry

3.1 Geometry of Satellites

It is clear that a geometric stereo model needs to be analyzed with respect to the relationship between the stereo acquisition geometry and the geometric accuracy in a variable geometric environment (Cain, 1989). There are some kinds of parameters to express the geometry. The B/H ratio is the ratio of the length between the two satellites to the average flying altitude above ground level. The B/H ratio has been widely used in the aerial triangulation. However, the B/H ratio is not appropriate as a measure of the geometry for the satellite stereo models which should consider the curvature of the earth (Li, 2008). The RA is the angle that represents how much the epipolar plane rotates about flight line. The CA is the angle between the two rays in the convergence or epipolar plane. An angle between 30 and 60 degrees is ideal. The AA is the apparent offset from the centre view that a stereo pair has and should be under 20 deg (GEOIMAGE, 2010).

We used only B/H ratio and BIE that are the important parameters related to the accuracy of satellite stereo models (Zhu, 2008) . Figure 3 shows the geometry of two satellites which is used in this study. We set up a local Cartesian coordinate system where the origin is the centre of the scene. S_1 and S_2 are the positions of two satellites. H is the altitude of the satellite orbit above ground level, R is the radius of the earth, e_i is the elevation of the satellite i, and Az_i is the azimuth of the satellite i. We can find the positions of two satellites in (10) and (11).

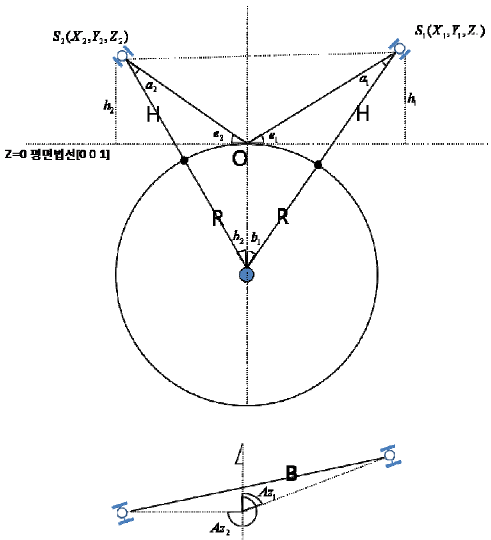

Figure 3. Geometry of Satellites

$$S_1 = \begin{pmatrix} X_1 \\ Y_1 \\ Z_1 \end{pmatrix} = \begin{pmatrix} OS_1 \cdot \cos e_1 \cdot \sin Az_1 \\ OS_1 \cdot \cos e_1 \cdot \cos Az_1 \\ OS_1 \cdot \sin e_1 \end{pmatrix} \quad (10)$$

$$S_2 = \begin{pmatrix} X_2 \\ Y_2 \\ Z_2 \end{pmatrix} = \begin{pmatrix} OS_2 \cdot \cos e_2 \cdot \sin Az_2 \\ OS_2 \cdot \cos e_2 \cdot \cos Az_2 \\ OS_2 \cdot \sin e_2 \end{pmatrix} \quad (11)$$

Baseline (B) and B/H ratio can be derived by formulas (12) and (13).

$$B = \text{length}(\overline{S_1S_2}) = \sqrt{(X_1 - X_2)^2 + (Y_1 - Y_2)^2 + (Z_1 - Z_2)^2} \quad (12)$$

$$B/H \text{ ratio} = \frac{B}{\frac{h_1+h_2}{2}} \quad (13)$$

Equation (14) shows how we calculate BIE.

$$u_1 = \frac{\overrightarrow{OS_1}}{|\overrightarrow{OS_1}|}, \quad u_2 = \frac{\overrightarrow{OS_2}}{|\overrightarrow{OS_2}|}$$

$$BIE = \sin^{-1}\left(\frac{\overrightarrow{u_1}+\overrightarrow{u_2}}{|\overrightarrow{u_1}+\overrightarrow{u_2}|} \cdot \vec{z}\right) \quad (14)$$

3.2 Bias of pixel in forward RPC

Biases in RPCs generated from sensor orientation, which are generally attributed to small systematic errors in gyro and star tracker recordings, have been shown to be adequately modeled by zero-order shifts in image space (Fraser, 2009). Figure 3 shows these biases quantified by differences between computing image coordinates via the RPCs and measured image coordinates of the GPS points. It can be seen that, although the mean of discrepancies are -0.4 ~ 3.8 pixels, the standard errors of differences are less than 0.37 pixels. This instance is to show that compensating image biases inherent in RPCs can increase geopositioning accuracies.

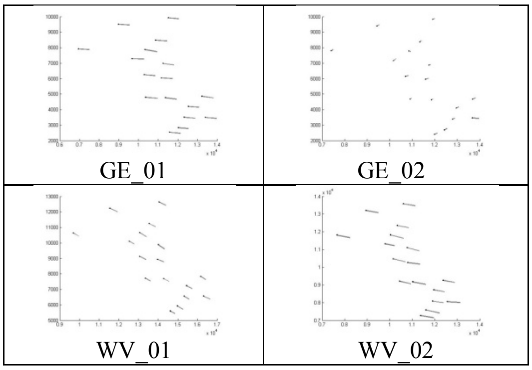

Figure 3. Bias vectors of image coordinates

Images	RMSE		MEAN		S.D.	
	Line	Sample	Line	Sample	Line	Sample
GE_01	3.846	0.440	3.842	-0.398	0.188	0.194
GE_02	0.861	0.535	0.781	0.450	0.373	0.297
WV_01	2.049	1.360	2.029	-1.345	0.300	0.206
WV_02	3.625	0.873	3.612	-0.840	0.312	0.245

Table 2. Biases of the image coordinates

3.3 Accuracy of Stereo Models

Figure 4 shows ground coordinate biases in RPC sensor orientation for the homo- and hetero-type stereo models without GCPs. The worst systematic bias errors in object points of -0.3m in easting and -2.1m in northing at the 'GE_01 and WV_02' stereo pair and 2.2m in height at the 'GE_01 and GE_02' stereo pair resulted. In any case of all six stereo pairs, there are shift bias patterns in both planimetry and height regardless of homo-type or hetero-type stereos.

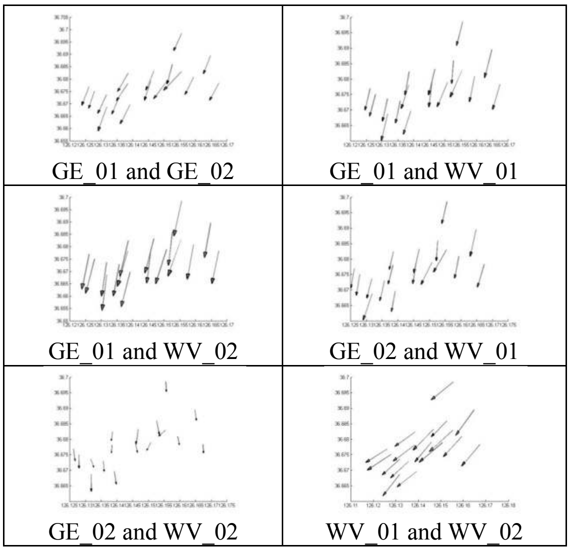

Figure 4. Residuals of stereo models without GCPs

Figure 5 shows the residuals of the six stereo models using single GCP(#37) located in the middle of the test area. Only one GCP compensates bias error efficiently and the accuracies are remarkably improved to 0.39 meters in CEP(90) and 0.62 meters in LEP(90). However, the random errors exist in the RPC models provided with the GCP.

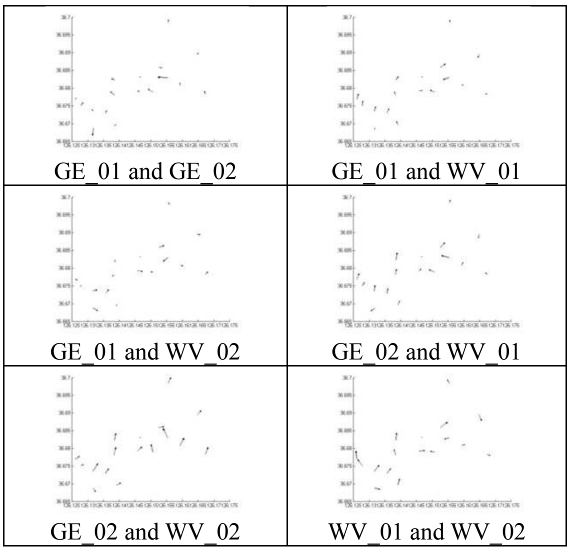

Figure 5. Residuals of stereo models with single GCP

Figure 6 shows ground coordinate biases in RPC sensor orientation for the six stereo models using four well distributed GCPs(#9, #11, #61, #100). The accuracy of this case has a strong resemblance to that of the single GCP.

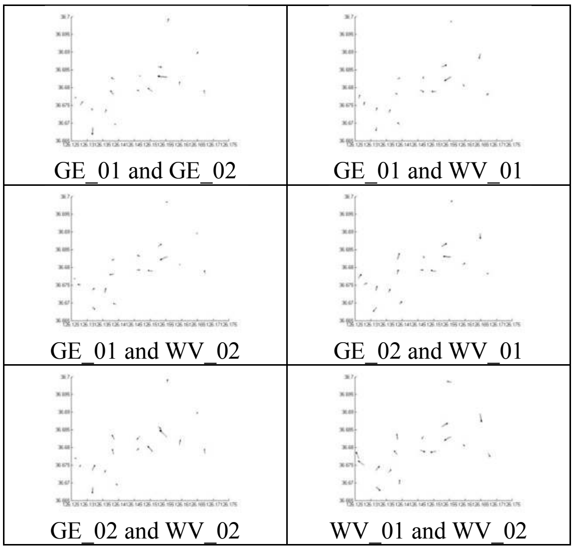

Figure 6. Residuals of stereo models with four GCPs

3.4 Results and Discussions

Table 3 shows the results of our investigation. The geometric accuracy is assessed in planimetry and height using no GCP, 1 GCP, and 4 GCP respectively. The accuracy of stereo models dramatically improved with only one GCP, however when we used more GCPs, the accuracy slightly increased. Regarding stereo types, it was concluded that there is no significant difference in accuracy between homo-type and hetero-type stereo pairs if they have good stereo geometry such as B/H, and BIE. In the case of 'GE_02 and WV_02' hetero-type stereo pair, planimetry accuracy without GCP is the best.

Image pairs	B/H	BIE	No GCP		1 GCP		4 GCPs	
			CEP (90)	LEP (90)	CEP (90)	LEP (90)	CEP (90)	LEP (90)
GE_01 & GE_02	0.74	79.3	1.33	2.53	0.25	0.53	0.25	0.62
GE_01 & WV_01	1.16	81.4	1.35	2.07	0.24	0.41	0.21	0.38
GE_01 & WV_02	0.69	79.9	2.25	0.76	0.20	0.38	0.19	0.46
GE_02 & WV_01	0.61	61.3	1.24	2.13	0.30	0.48	0.26	0.53
GE_02 & WV_02	0.73	78.3	0.69	1.56	0.39	0.62	0.29	0.51
WV_01 & WV_02	0.71	65.5	1.60	2.39	0.37	0.57	0.33	0.58

Table 3. Accuracy of Stereo Models

4. CONCLUSION

In this study, GeoEye-1 in-track stereo pair and WorldView-2 in-track stereo pair were collected in the same region. We compared the three-dimensional geopositioning accuracy of different combinations from these four images. According to the results in table 3, the following conclusions can be confirmed.

- In-track stereo pairs of GeoEye-1 and WorldView-2 are meaningfully accurate for developing geo-spatial information for a map of 1/5,000 without any GCPs.
- The accuracies of hetero-type stereo pairs which have good geometry(B/H and BIE) are as accurate as that of homo-type in-track stereo pairs.
- The hetero-type stereo pair model of the images with different ground sample distances could be comparatively accurate, because RPC model is independent on sensors.

References :

Cain, J. 1989, Stereomodel Acquisition Geometry, Ph.D. thesis, U.C. Berkeley.

Fraser, C.S. and Hanley, H.B., 2003. Bias Compensation in Rational Functions for Ikonos Satellite Imagery, Photogrammetric Engineering & Remote Sensing, 69(1), pp. 53-57

Fraser, C.S. and Ravanbakhsh, M., 2009. Georeferencing accuracy of GeoEye-1 imagery, Photogrammetric Engineering & Remote Sensing, 75(6), pp. 634- 640.

GEOIMAGE, 2010, "Digital Elevation Models from Satellite Imagery".
http://www.geoimage.com.au/geoimage/uploads/Geoimage_DEM_brochure_Oct10_small_lowres.pdf

Grodecki, J. and Dial, G., 2003. Block adjustment of high-resolution satellite images described by rational polynomials, Photogrammetric Engineering & Remote Sensing, 69(1), pp. 59-68.

Li, J., Shao, Y., Wang, J., and Yang, J.(2008), The Research and Design of The Base-Height Ratio for the Three Linear Array Camera of Satellite Photogrammetry, The International Archives of the Photogrammetry, Remote Sensing and Spatial Information Sciences, Vol. XXXVII.Part B1.Beijing, pp. 757-760

Li, R., Zhou, F., Niu, X., and Di, K., 2007. Integration of Ikonos and QuickBird Imagery for Geopositioning Accuracy Analysis, Photogrammetric Engineering & Remote Sensing, 73(9), pp. 1067-1074.

NIMA, 2000, The Compendium of Controlled Extensions for the National Imagery Transmission Format, ver. 2.1.

Toutin, T., 2004. DTM Generation from Ikonos In-Track Stereo Images Using a 3D Physical Model, Photogrammetric Engineering & Remote Sensing, 70(6), pp. 695–702.

Zhu, L., Umakawa, H., Guan, F., Tachibana, K., and Shimamura, H., 2008. Accuracy Investigation of Orthoimages Obtained from High Resolution Satellite Stereo Pairs, The International Archives of the Photogrammetry, Remote Sensing and Spatial Information Sciences, Beijing, Vol. XXXVII. Part B1. pp.1145-1148